RESEARCH ARTICLE

Figures and figure supplements

Antagonistic control of *Caenorhabditis elegans* germline stem cell proliferation and differentiation by PUF proteins FBF-1 and FBF-2

Xiaobo Wang *et al*

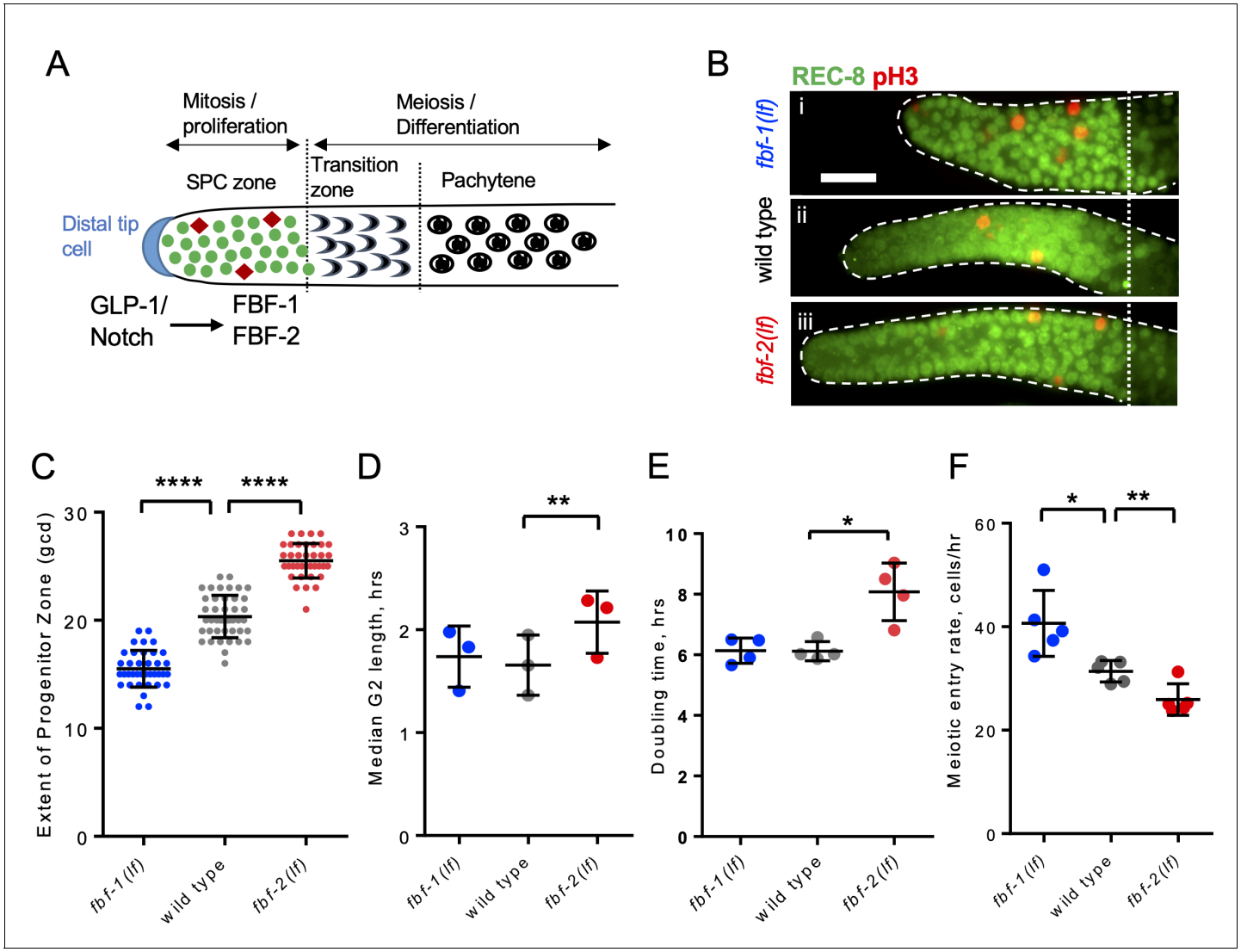

Figure 1. FBF-1 and FBF-2 differentially regulate the extent of germline stem and progenitor cell (SPC) zone. (**A**) Schematic of the distal germline of *C. elegans* adult hermaphrodite. In this and following images, germlines are oriented with their distal ends to the left. GLP-1/Notch signaling from the distal tip cell (blue) supports germline SPC proliferation. Progenitors enter meiosis in the transition zone. FBF-1 and FBF-2, downstream of GLP-1/Notch, are required for SPC maintenance. Green circles, stem and progenitor cells; red diamonds, mitotically dividing cells. (**B**) Distal germlines dissected from adult wild type, *fbf-1(lf)*, and *fbf-2(lf)* hermaphrodites and stained with anti-REC-8 (green) and anti-phospho-Histone *H3* (pH3; red) to visualize the SPC zone and mitotic cells in M-phase. Germlines are outlined with the dashed lines and the vertical dotted line marks the beginning of transition zone as recognized by the 'crescent-shaped' chromatin and loss of REC-8. Scale bar: 10 μm. (**C**) SPC zone lengths of the wild type, *fbf-1(lf)* and *fbf-2(lf)* germlines were measured by counting germ cell diameters (gcd) spanning SPC zone. Genetic background is indicated on the X-axis and the extent of SPC zone on the Y-axis. Differences in SPC zone lengths were evaluated by one-way ANOVA with Dunnett's post-test. Data were collected from three independent experiments, with 10–15 germlines per strain per replicate. (**D**) Median SPC G2-phase length in different genetic backgrounds, as indicated on the X-axis. Difference in median G2 length was evaluated by one-way ANOVA with Dunnett's post-test. G2 length was estimated in three independent experiments as shown in ***Figure 1—figure supplement 1C***, each replicate experiment involved analysis of 145–159 germlines per strain. (**E**) Larval germ cell doubling time in different genetic backgrounds (as indicated on the X-axis). Plotted values are individual data points and means ± SD. Difference in germ cell doubling time was evaluated by one-way ANOVA with Dunnett's post-test. Data were collected from four independent replicates as shown in ***Figure 1—figure supplement 1E,F***, each analyzing 15–21 germlines per strain per time point (144–148 germlines per strain total). (**F**) Meiotic entry rate of germline progenitors in different genetic backgrounds indicated on the X-axis. Differences in meiotic entry rate between each *fbf* and the wild type were evaluated by one-way ANOVA with T-test with Bonferroni correction post-test. Meiotic entry rates were estimated in five independent experiments as shown in ***Figure 1—figure supplement 1G***, each analyzing 5–7 germlines per strain per time point (89–94 germlines per strain total). (**B–F**) All experiments were performed at 24˚C. Plotted values are individual data points and means ± SD. Asterisks mark statistically significant differences (****, $p<0.0001$; **, $p<0.01$; *, $p<0.05$).

Figure 1—figure supplement 1. SPC dynamics in different genetic backgrounds. (**A**) SPC zone length measured as the germ cell diameters (gcd) spanning the stem and progenitor cell zone. X-axis: the time after release of synchronized L1s from starvation. 46 hr, young adult; 52 hr, adult; 63 hr,

Figure 1—figure supplement 1 continued on next page

Figure 1—figure supplement 1 continued

second day adult. Plotted values are means ± S.D. 10–12 germlines were scored for each genotype at each time point. (**B**) Quantification of mitotic indices of germline SPCs in the genetic backgrounds indicated on the X-axis. Differences in mitotic indices were evaluated by one-way ANOVA with Dunnett's post-test. Data were collected from two independent experiments and 10 germlines were scored for each genotype per replicate. (**C**) Representative time course of EdU labeling of mitotic cells in different genetic backgrounds in one biological replicate. X-axis displays the times when animals were dissected for staining for EdU and pH3. Y-axis indicates the percent of pH3-positive germ cells that are also EdU positive. Plotted values are means ± SD. 6–14 germlines were analyzed for each genotype per time point in each replicate. The median G2 lengths were interpolated as the times when 50% of nuclei in M phase (pH3-positive) were labeled with EdU. (**D**) S-phase indices of germline SPCs in different genetic backgrounds as indicated on the X-axis. Differences in S-phase indices were evaluated by one-way ANOVA with Dunnett's post-test. Data were collected from three independent experiments with 7–10 germlines scored for each genotype per replicate. (**E**) Representative images of germ cells in the indicated genetic backgrounds and conditions. Germ cells are visualized using a germ-cell-specific marker PGL-1::GFP. Scale bar, 5 μm. (**F**) Quantification of larval germ cell proliferation in different genetic backgrounds. A representative time course of one biological replicate, plotted values are means ± SD. 15–21 larvae per genotype were analyzed for each time point. (**G**) Meiotic entry rate of progenitors in different genetic backgrounds. Representative time course of accumulating EdU-labeled, REC-8-negative germ cells in different genetic backgrounds in one biological replicate. X-axis displays time points when animals were dissected for staining for EdU and REC-8. Y-axis indicates the number of EdU-positive cells that are negative for REC-8. Plotted values are means ± SD. 5–7 germlines were scored for each genotype at each time point in each individual biological replicate, resulting in analysis of 89–94 total germlines per strain over five replicates. The data were fit to linear regression models, R values were between 0.87 and 0.94. The rates of meiotic entry were determined as the slopes of the regression lines. (**A–G**) All experiments were performed at 24°C.

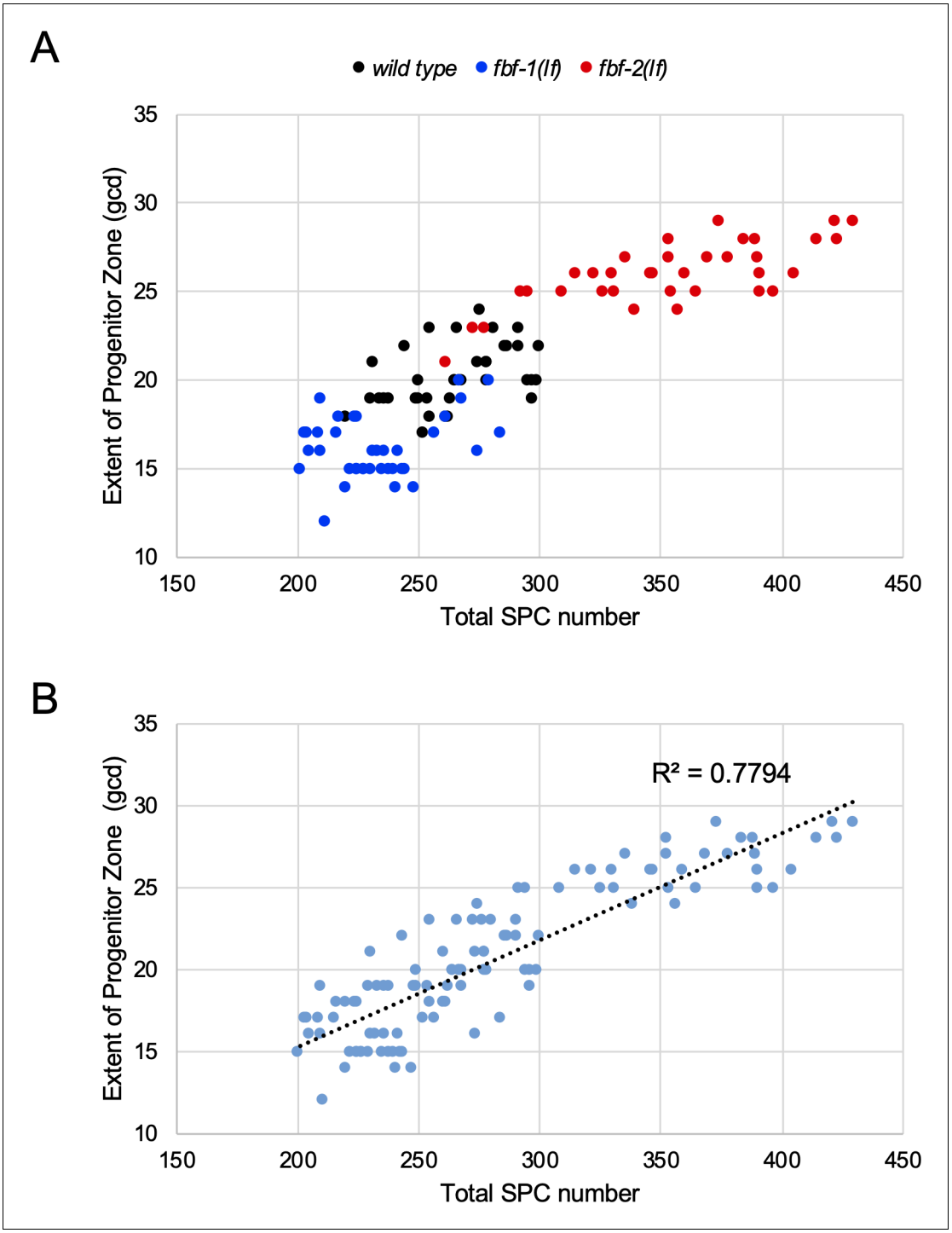

Figure 1—figure supplement 2. The number of SPC cell rows is a robust estimate of progenitor numbers. (**A**) SPCs were counted in germlines of the wild type, *fbf-1(lf)*, and *fbf-2(lf)* adults reared at 24°C; in parallel the lengths of SPC zones were measured as the number of REC-8-positive cell diameters. The SPC zone length (gcd) is plotted against the number of SPCs in each germline. The data represent three biological replicates for each strain. (**B**) Linear regression analysis performed on merged data from A shows robust correlation between the SPC number and SPC zone length in the three genetic backgrounds analyzed (R^2 = 0.7794).

Figure 2. FBF-mediated repression of cyclin B limits accumulation of germline progenitor cells. (**A**) Schematic representation of transgenes encoding 3xFLAG-tagged CYB-2.1(wt) with wild type FBF binding elements (FBEs, UGUxxxAU) in 3'UTR and 3xFLAG-tagged CYB-2.1(fbm) with *F*BF *b*inding elements *m*utated (ACAxxxAU). (**B**) qRT-PCR of *3xflag::cyb-2.1* and *unc-54* transcripts in *3xflag::cyb-2.1(wt)* and *3xflag::cyb-2.1(fbm)* worms using actin (*act-1*) as a normalization control. Data represent two replicates, values are average ± SD. Differences in levels were evaluated by T-test; asterisks mark statistically significant difference (p<0.001). (**C**) Immunoblot analysis of 3xFLAG::CYB-2.1 protein levels in *3xflag::cyb-2.1(wt)* and *3xflag::cyb-2.1(fbm)* worms using α-tubulin as a loading control. Data represent three replicates, values are average ± SD. Differences in levels were evaluated by T-test;

Figure 2 continued on next page

Figure 2 continued

asterisk marks statistically significant difference (p<0.05). (**D**) Larval germ cell doubling time in different genetic backgrounds (as indicated on the X-axis). Plotted values are individual data points and means ± SD. Difference in germ cell doubling time was evaluated by one-way ANOVA with Dunnett's post-test. (**E**) Meiotic entry of progenitors in different genetic backgrounds. Time course of accumulating EdU-labeled, REC-8 negative germ cells in different genetic backgrounds in one biological replicate (the data are representative of two biological replicates, each analyzing 6–7 germlines per strain per time point, up to 41–42 germlines per strain total). X-axis displays time points when animals were dissected for staining for EdU and REC-8. Y-axis indicates the number of EdU-positive cells that are negative for REC-8. Plotted values are means ± SD. (**F**) Distal germlines dissected from the *fbf-2(lf), fbf-2(lf); cyb-2.1(fbm)* and *fbf-2(lf); cyb-2.1(wt)* animals and stained with anti-REC-8 (green) and anti-pH3 (red). Germlines are outlined with dashed lines and the vertical dotted line marks the beginning of transition zone. Scale bar: 10 μm. (**G**) The extent of SPC zone in the *fbf-2(lf), fbf-2(lf); cyb-2.1(fbm)* and *fbf-2(lf); cyb-2.1(wt)* genetic backgrounds. Plotted values are individual data points and means ± SD. Differences in SPC zone lengths were evaluated by one-way ANOVA with Dunnett's post-test; asterisks mark statistically significant difference (p<0.0001). Data were collected from two independent experiments and 14–19 germlines were scored for each genotype per replicate. (**H**) The extent of SPC zone in the *fbf-2(lf); cyb-2.1(fbm)* after *cyb-2.1(RNAi)* compared to the empty vector RNAi control. Plotted values are individual data points and means ± SD. Differences in SPC zone lengths were evaluated by T-test; asterisks mark statistically-significant difference (p<0.0001). Data were collected from two independent experiments and 44 independent germlines were scored for each condition. (**I**) Immunoblot analysis of 3xFLAG::CYB-2.1 protein levels in *3xflag::cyb-2.1fbm* after *cyb-2.1(RNAi)* compared to the empty vector RNAi control. Tubulin was used as a loading control. (**B–I**) All experiments were performed at 15˚C.

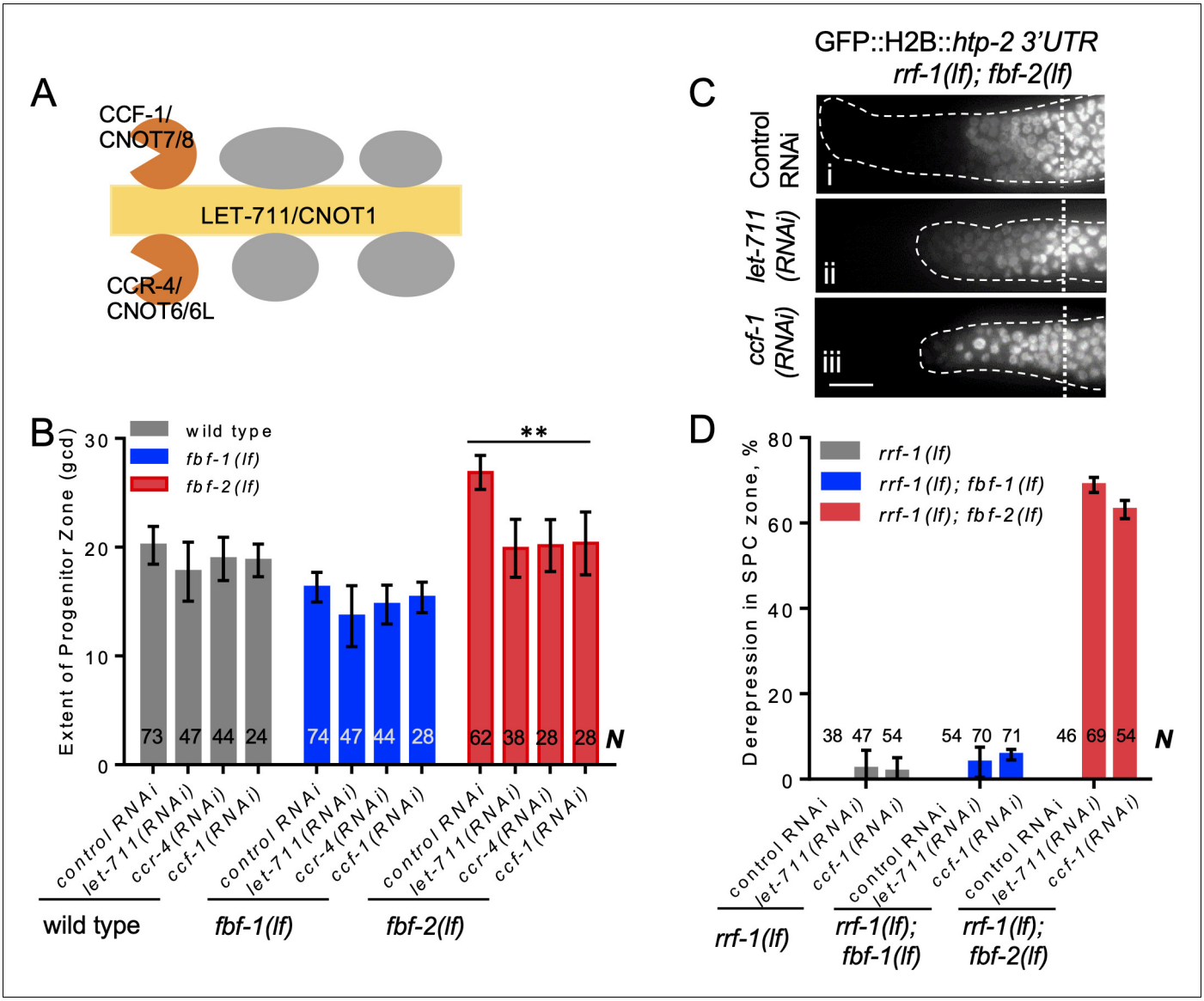

Figure 3. CCR4-NOT deadenylase complex promotes FBF-1 function in germline SPCs. (**A**) Schematic of CCR4-NOT deadenylase complex in humans and *C. elegans*; highlighted are the scaffold (yellow) and catalytic (orange) subunits targeted by RNAi in this study. (**B**) The extent of SPC zone after knocking down CCR4-NOT subunits in the wild type, *fbf-1(lf)* and *fbf-2(lf)* genetic backgrounds. Genetic backgrounds and RNAi treatments are indicated on the X-axis and the average size of SPC zone ± SD is plotted on the Y-axis. Differences between CCR4-NOT RNAi and the empty vector RNAi control were evaluated by one-way ANOVA. Asterisks mark the group with significant changes in SPC zone length after CCR4-NOT knockdown, $p<0.01$. Data were collected from three independent experiments. N, the number of hermaphrodite germlines scored. (**C**) Distal germlines of *rrf-1(lf); fbf-2(lf)* expressing a GFP::Histone H2B fusion under the control of the *htp-2* 3'UTR after the indicated RNAi treatments. Germlines are outlined with dashed lines and vertical dotted lines indicate the beginning of the transition zone. All images were taken with a standard exposure. Scale bar: 10 μm. (**D**) Percentage of germlines showing expression of GFP::H2B fusion extended to the distal end in the indicated genetic backgrounds and knockdown conditions. Plotted values are means ± SD. Data were collected from three independent experiments. *N*, the number of germlines scored. Efficiencies of RNAi treatments were confirmed by sterility (***Figure 3—figure supplement 1B***) or embryonic lethality (***Supplementary file 3***). (**B–D**) All experiments were performed at 24˚C.

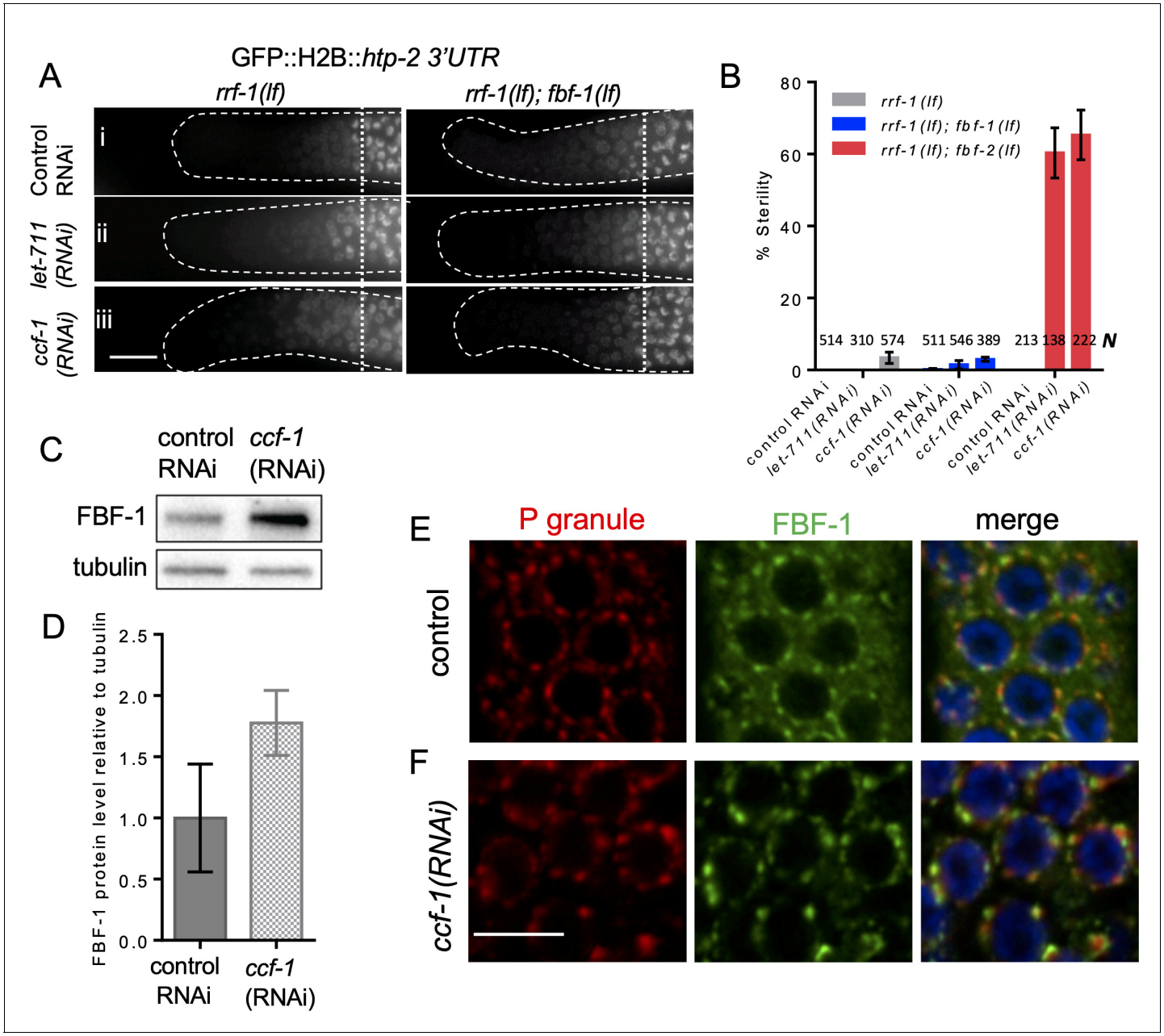

Figure 3—figure supplement 1. CCR4-NOT deadenylase complex promotes FBF-1 function in germline SPCs. (**A**) Distal germlines of *rrf-1(lf)* and *rrf-1 (lf); fbf-1(lf)* expressing GFP::Histone H2B fusion under the control of the *htp-2* 3'UTR after the indicated RNAi treatments. Genetic backgrounds are indicated on top of each image column. Germlines are outlined with dashed lines and vertical dotted lines indicate the beginning of the transition zone. All images were taken with a standard exposure. Scale bar: 10 μm. Efficiencies of RNAi treatments were assessed by sterility (panel B) or embryonic lethality (***Supplementary file 3***). (**B**) Percentage of sterile worms after a knockdown of CCR4-NOT subunits in *rrf-1(lf), rrf-1(lf); fbf-1(lf)* and *rrf-1(lf); fbf-2(lf)* genetic backgrounds. Data were collected from three independent experiments. *N*, the number of hermaphrodites scored. (**C**) A representative western blot detecting endogenous FBF-1 following *ccf-1(RNAi)*. Tubulin is used as a control. (**D**) Endogenous FBF-1 protein levels following *ccf-1(RNAi)* determined by densitometry of the western blot results from three independent experiments normalized to tubulin. Plotted values are means ± SD. (**E, F**) Confocal images of germline SPC zone co-immunostained for endogenous FBF-1 (green) and P granules (red) in empty vector RNAi control germlines (**E**) and after *ccf-1* knockdown (**F**). Scale bar: 5 μm. (**A–F**) All experiments were performed at 24°C.

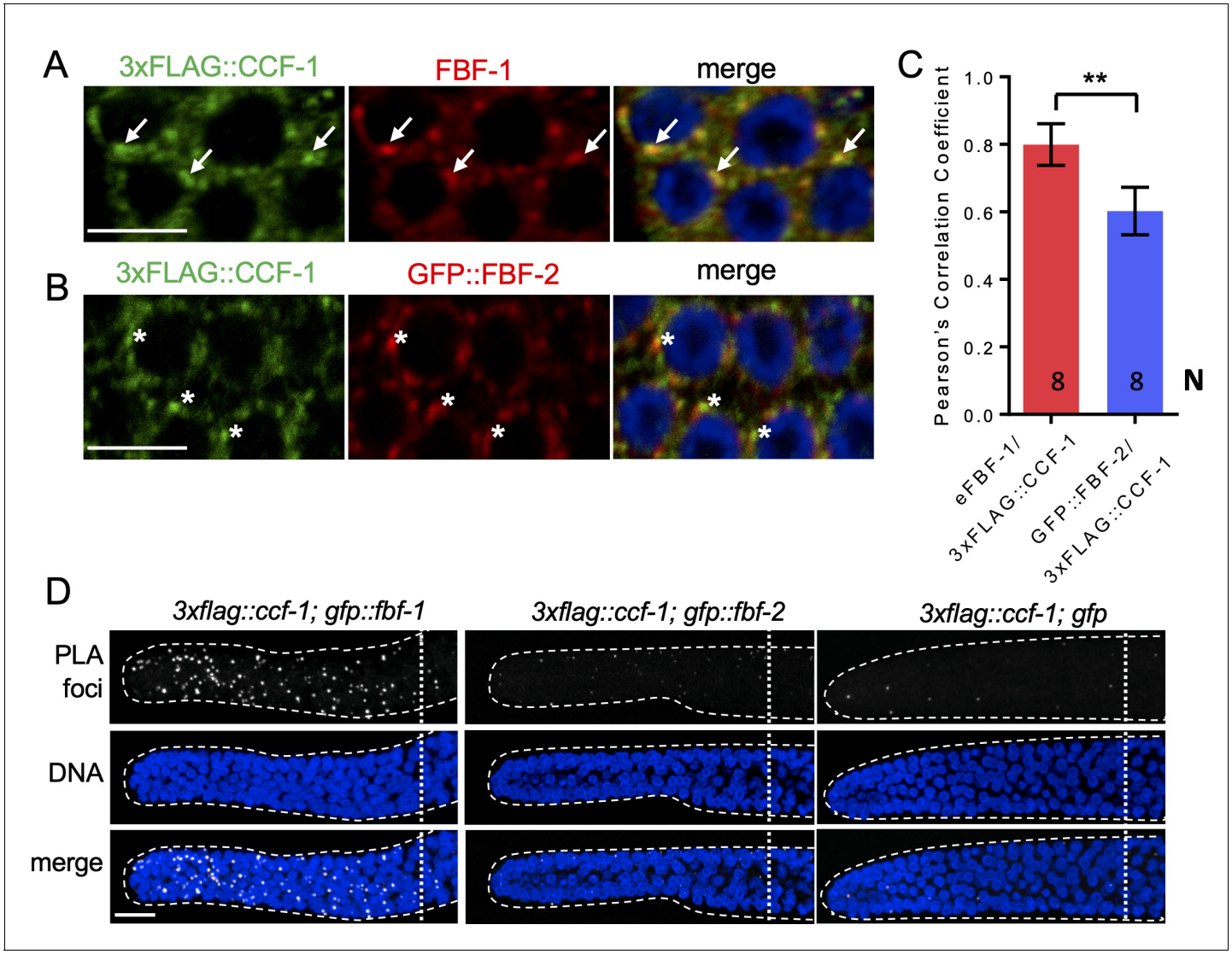

Figure 4. FBF-1 colocalizes with CCR4-NOT complex in germline SPCs. (**A–B**) Confocal images of SPCs co-immunostained for endogenous FBF-1 (**A**) or GFP-tagged FBF-2 (B, red) and 3xFLAG-tagged CCF-1 (green). DNA staining is in blue (DAPI). Arrows indicate complete overlap of FBF-1 and CCF-1 granules. Asterisks denote FBF-2 granules localizing close but not overlapping with CCF-1 granules. Scale bars in A and B: 5 µm. (**C**) Pearson's correlation analysis quantifying the colocalization between FBF and CCF-1 granules in co-stained germline images. Plotted values are means ± SD. *N*, the number of analyzed germline images (single confocal sections through the middle of germline SPC nuclei including 5–8 germ cells). Asterisks mark statistically significant difference by Student's t-test, $p<0.01$. (**D**) Confocal images of the distal germline SPC zones with PLA foci (grayscale) and DNA staining (blue). Germlines are outlined with dashed lines and vertical dotted lines indicate the beginning of the transition zone. Genotypes are indicated on top of each image group. Scale bar: 10 µm. (**A–D**) All experiments were performed at 24˚C.

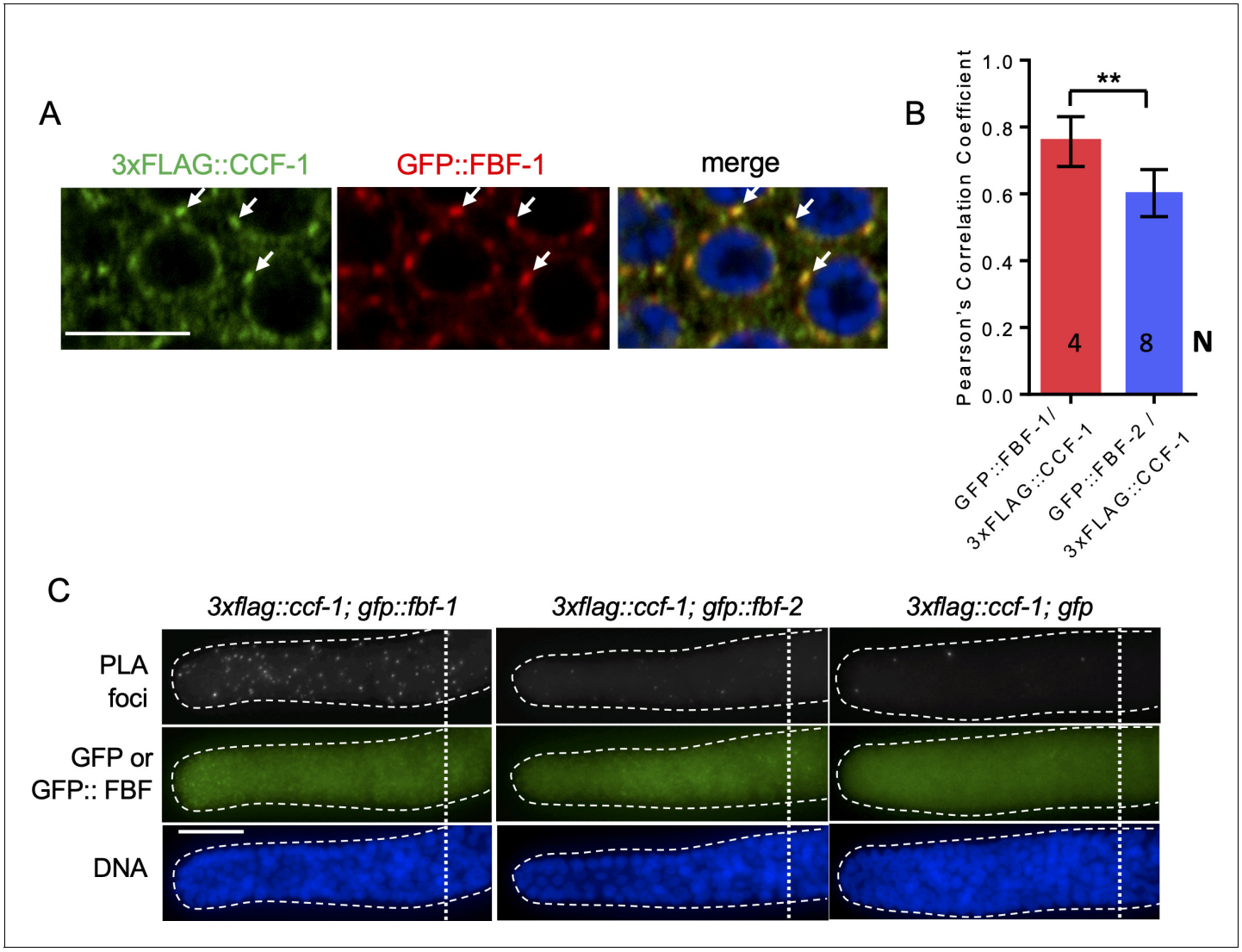

Figure 4—figure supplement 1. FBF-1 colocalizes with CCR4-NOT complex in germline SPCs. (**A**) Confocal images of SPCs co-immunostained for GFP::FBF-1(red) and FLAG::CCF-1 (green). DNA staining (DAPI) is in blue. Arrows indicate complete overlap of FBF-1 and CCF-1 granules. Scale bar: 5 µm. (**B**) Pearson's correlation analysis of the colocalization between GFP::FBF-1 and FLAG::CCF-1 granules in four single confocal sections compared to GFP::FBF-2/FLAG::CCF-1. Plotted values are means ± SD. Statistical analysis was performed by Student's t-test; asterisks mark statistically significant difference, $p<0.01$. The values for GFP::FBF-2/FLAG::CCF-1 colocalization are same as in ***Figure 4C***. (**C**) Epifluorescent images showing PLA signals (greyscale) and expression of GFP::FBF-1, GFP::FBF-2, and GFP alone (green) in SPCs. DNA staining is in blue (DAPI). Genotypes are indicated above each image group. Scale bar: 10 µm. (**A–C**) All experiments were performed at 24˚C.

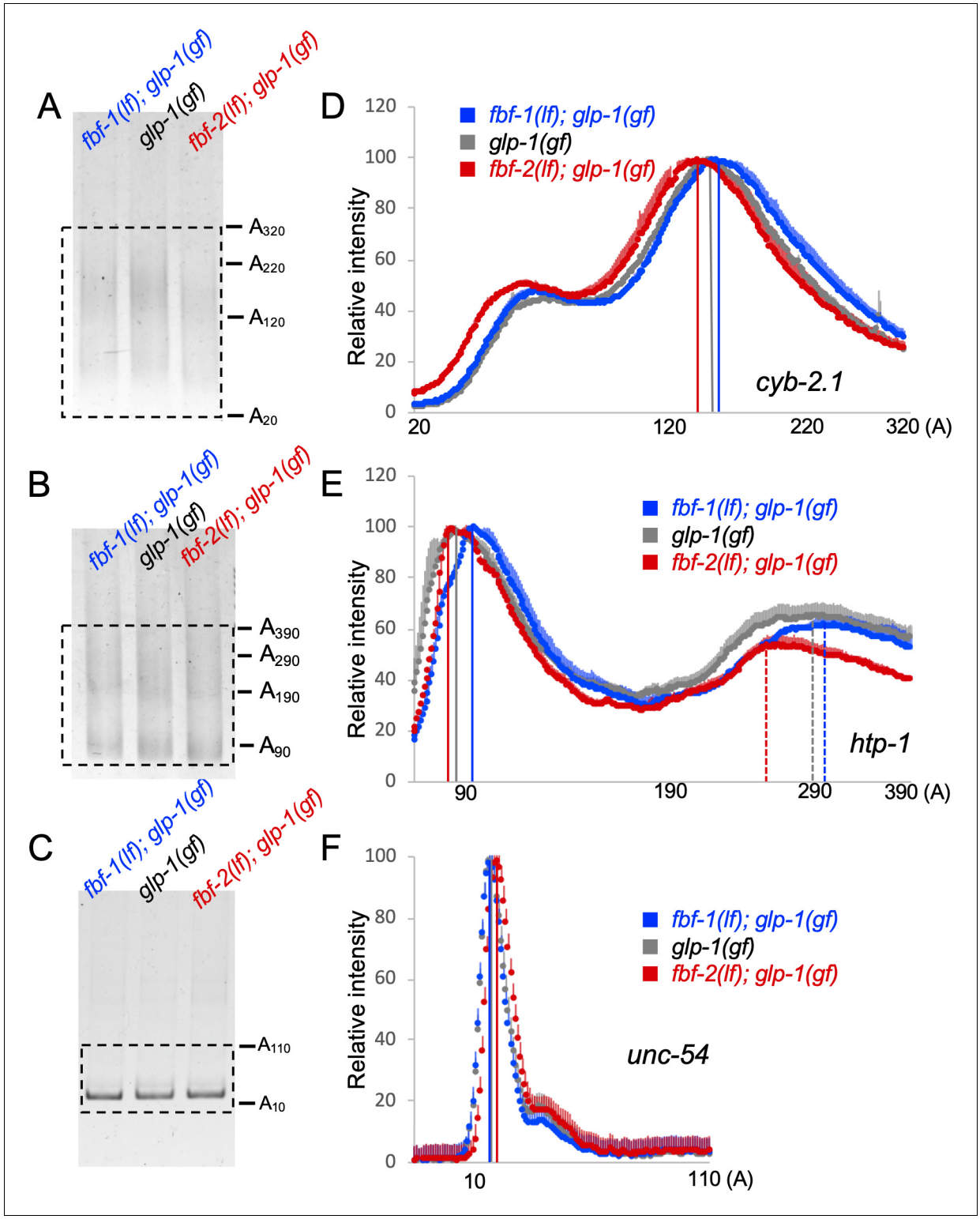

Figure 5. Antagonistic effects of FBF-1 and FBF-2 on poly(A) tail of target mRNAs. (**A–C**) Representative PAT-PCR amplification of the poly(A) tail of *cyb-2.1* (**A**), *htp-1* (**B**) and control myosin heavy chain *unc-54* (**C**) in *fbf-1(lf); glp-1(gf)*, *glp-1(gf)*, and *fbf-2(lf); glp-1(gf)* genetic backgrounds at 25°C. The estimated lengths of poly(A) tails based on the PCR fragment sizes are indicated on the right. The areas boxed by dotted lines were quantified by densitometry in ImageJ. (**D–F**) Densitometric quantification of PAT-PCR amplification products (boxed in A-C). Y-axis, mean relative intensity represents the average intensities of normalized PAT-PCR reactions from three independent biological replicates. X-axis, estimated sizes of poly(A) tails. Values are means + SD. Vertical lines in (**D–F**) mark the peaks of PAT-PCR intensity profiles for each mRNA in each genetic background, dashed lines mark secondary peaks for *htp-1*. (**A–F**) Nematodes for all replicates were grown at 25°C.

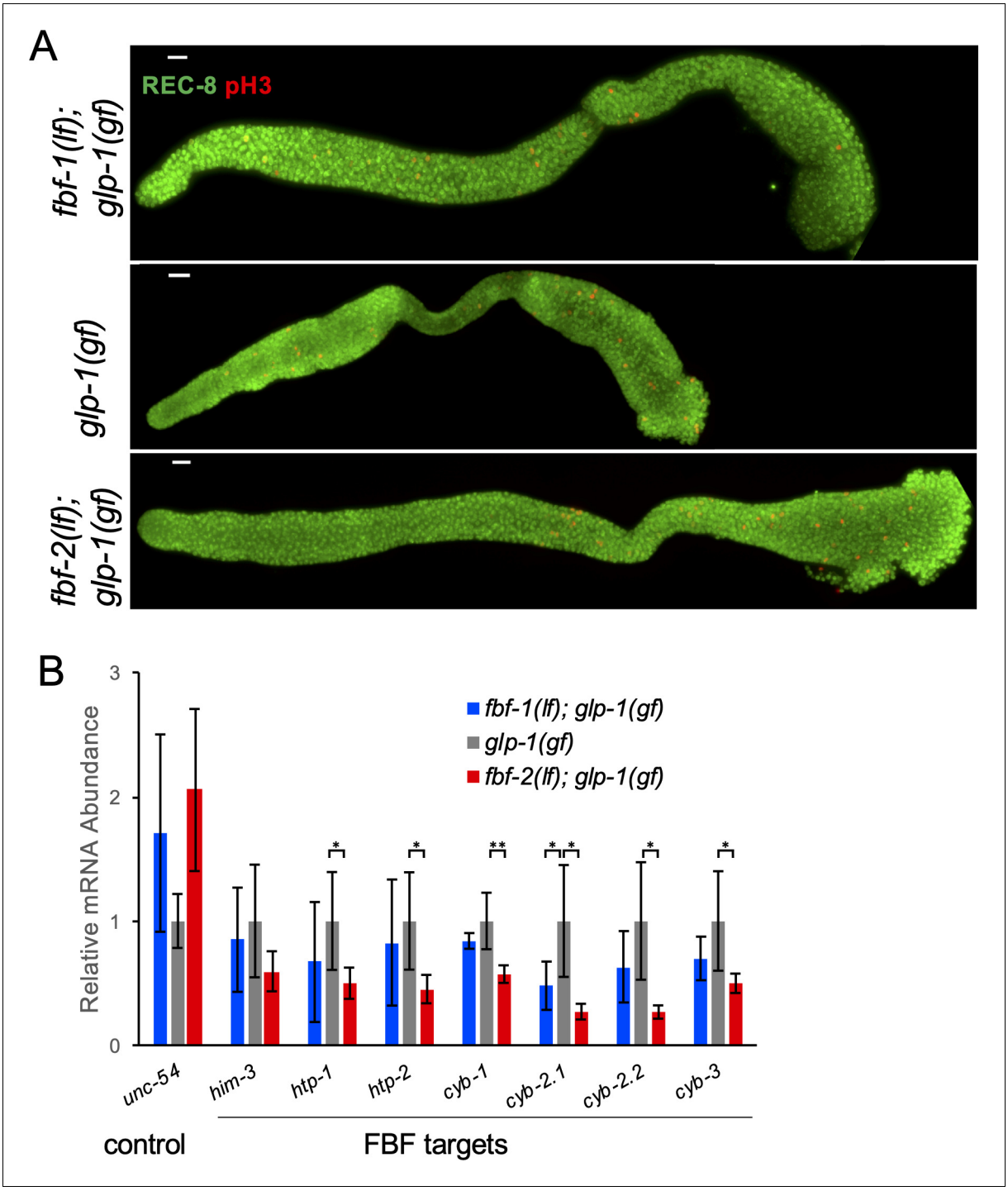

Figure 5—figure supplement 1. RNA analysis from predominantly mitotic germlines in *glp-1(gf)* genetic background. (**A**) Full germline tumors were observed in all *glp-1(gf)* strains grown at the restrictive temperature. Germlines dissected from *fbf-1(lf); glp-1(gf)*, *glp-1(gf)*, and *fbf-2(lf); glp-1(gf)* animals grown at 25˚C are stained with anti-REC-8 (green) and anti-pH3(red). Scale bars: 10 μm. (**B**) Steady-state mRNA abundance of FBF target genes and a control non-FBF target gene in *glp-1(gf); fbf-1(lf)*, *glp-1(gf)*, and *glp-1(gf); fbf-2(lf)* genetic backgrounds at 25˚C was determined by qRT-PCR and normalized to the levels of actin (*act-1*). Tested FBF target genes are associated with meiotic entry (*him-3*, *htp-1* and *htp-2*) or cell cycle regulation (*cyb-1*, *cyb-2.1*, *cyb-2.2* and *cyb-3*). The control gene is a myosin heavy chain, *unc-54*. Reported abundance represents the mean ± SD of the following number of independent biological replicates: three for *glp-1(gf)*, four for *fbf-2(lf); glp-1(gf)*, and six for *fbf-1(lf); glp-1(gf)*. Differences in mRNA abundance between *fbf-2(lf)* mutants and control were evaluated by one-way ANOVA tests with Student's t-test post-test; asterisks mark statistically significant differences (**, $p<0.01$; *, $p<0.05$). (**A–B**) All experiments were performed at 25˚C.

Figure 6. Three variable regions of FBF-2 prevent its cooperation with CCR4-NOT. (**A**) Schematics of FBF-1, FBF-2 and GFP::FBF-2(vrm) mutant transgene (***Wang et al., 2016***). Red and blue boxes indicate variable regions distinguishing FBF-1 and FBF-2 respectively, grey box indicates the RNA-binding domain, and green box indicates GFP tag. (**B**) Distal germlines of the indicated genetic backgrounds stained with anti-REC-8 (green) and anti-pH3 (red). Germlines are outlined with the dashed lines, and the vertical dotted line marks the beginning of transition zone. Scale bar: 10 µm. (**C**) The extent of SPC zone in the indicated genetic backgrounds (on the X-axis). FBF protein(s) present in each genetic background are noted above each data set. Plotted values are individual data points and means ± SD. Differences in SPC zone length between *fbf-1(lf) fbf-2(lf); gfp::fbf-2(vrm)* and the other strains were evaluated by one-way ANOVA test with Dunnett's post-test; asterisks mark statistically significant differences (p<0.0001). Data were

Figure 6 continued on next page

Figure 6 continued

collected from three independent experiments and 24–28 germlines were scored for each genotype. (**D**) The extent of SPC zone was measured after crossing the GFP::FBF-2(vrm), GFP::FBF-1(wt) and GFP::FBF-2(wt) transgenes into *fbf-1(lf)* genetic background. As controls, SPC zone length was also measured in *fbf-1(lf)* and the wild type. Plotted values are individual data points and means ± SD. Data were collected from two independent experiments and 8–17 germlines were scored for each genotype per replicate. Differences in SPC zone length between *fbf-1(lf)* and all other strains were evaluated by one-way ANOVA test with Dunnett's post-test; asterisks mark statistically significant differences (****, $p<0.0001$; **$p<0.01$). (**E**) The extent of SPC zone after knocking down CCR4-NOT subunits in the *fbf-1(lf) fbf-2(lf); gfp::fbf-2(vrm)* genetic background. RNAi treatments are indicated on the X-axis and average length of SPC zone ± SD on the Y-axis. Differences in SPC zone length between CCR4-NOT knockdowns and control were evaluated by one-way ANOVA (asterisks, $p<0.01$). Data were collected from three independent experiments. *N*, the number of independent germlines scored. (**F**) Confocal images of the distal germline SPC zones with PLA foci (grayscale) and DNA staining (blue). Germlines are outlined with dashed lines and vertical dotted lines indicate the beginning of the transition zone. Genotypes are indicated on top of each image group. Scale bar: 10 μm. (**B–D**): All experiments were performed at 24˚C.

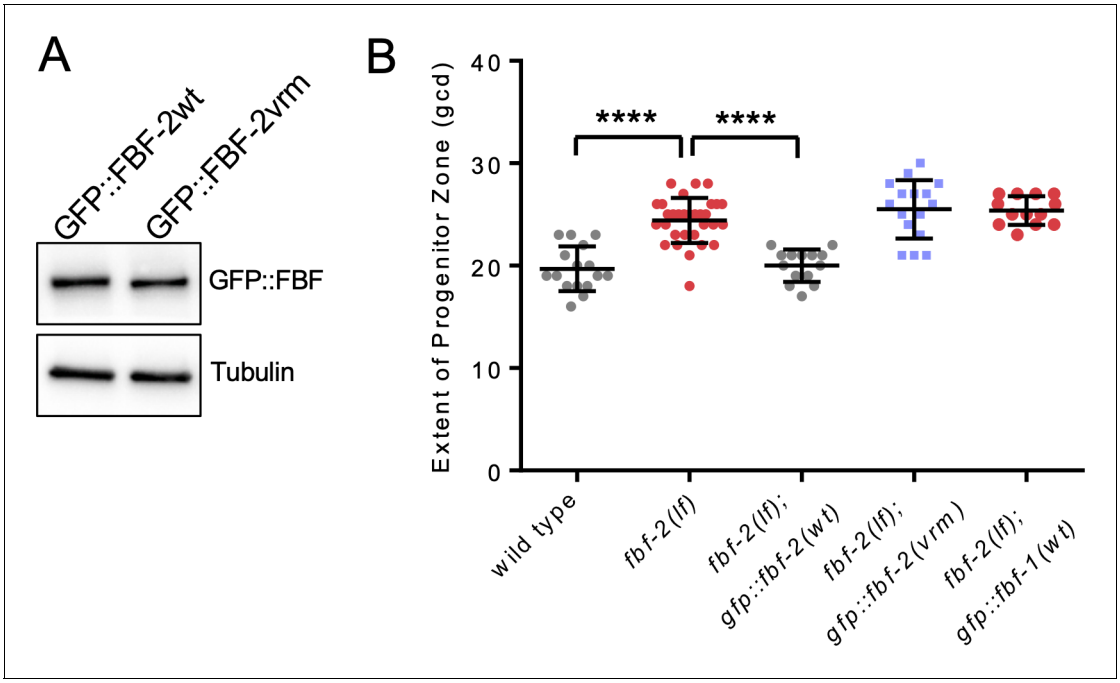

Figure 6—figure supplement 1. Variable regions 1, 2 and 4 of FBF-2 are required to rescue FBF-2-specific function in germline SPCs. (**A**) Expression levels of GFP::FBF-2(wt) and GFP::FBF-2(vrm) transgenes assessed by a western blot. Tubulin is used as a control. (**B**) The extent of SPC zone measured after crossing the GFP::FBF-2(vrm), GFP::FBF-2(wt) and GFP::FBF-1(wt) transgenes into *fbf-2(lf)* genetic background. As controls, SPC zone length was also measured in *fbf-2(lf)* and the wild type. Plotted values are individual data points and means ± SD. Differences in SPC zone length between *fbf-2(lf)* and other strains were evaluated by one-way ANOVA test with Dunnett's post-test; asterisks mark statistically significant differences (****, $p<0.0001$). Data were collected from two independent experiments and 6–16 germlines were scored for each genotype per replicate. (**A–B**) All experiments were performed at 24˚C.

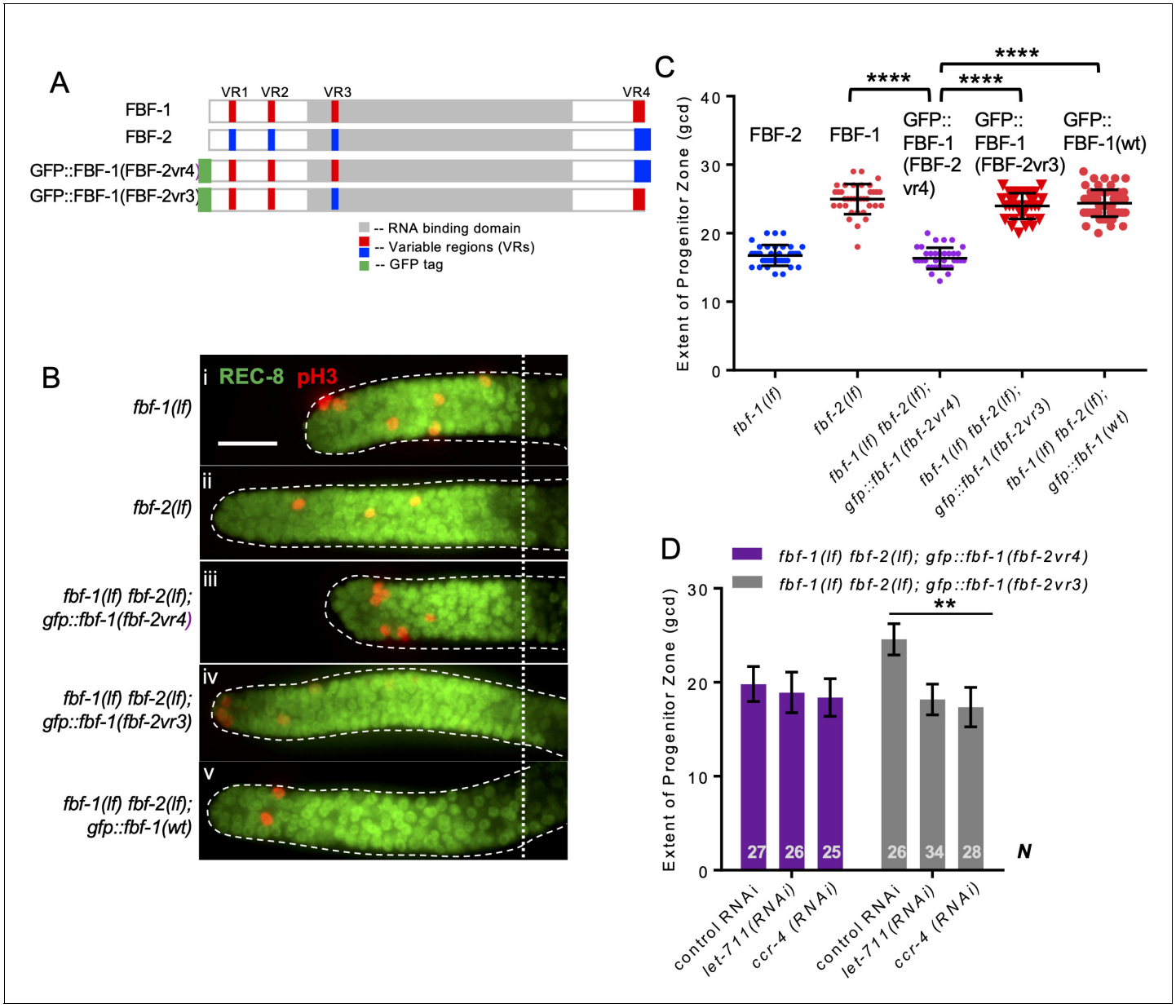

Figure 7. Variable region 4 (VR4) from FBF-2 is sufficient to prevent FBF-1 chimera from cooperation with CCR4-NOT. (**A**) Schematics of FBF-1, FBF-2, transgenic GFP::FBF-1(FBF-2vr4) chimera (with VR4 swapped from FBF-2), and transgenic GFP::FBF-1(FBF-2vr3) chimera (with VR3 swapped from FBF-2). Red and blue boxes, variable regions distinguishing FBF-1 and FBF-2 respectively; grey box, RNA-binding domain; green box, GFP tag. (**B**) Distal germlines dissected from the indicated genetic backgrounds stained with anti-REC-8 (green) and anti-pH3 (red). Germlines are outlined with the dashed lines and the vertical dotted line marks the beginning of the transition zone. Scale bar: 10 µm. (**C**) The extent of SPC zone in the indicated genetic backgrounds (on the X-axis). FBF protein present in each genetic background is noted above each data set. Plotted values are individual data points and means ± SD. Differences in SPC zone length between *fbf-1(lf) fbf-2(lf); gfp::fbf-1(fbf-2vr4)* and the other strains were evaluated by one-way ANOVA test with Dunnett's post-test; asterisks mark statistically significant differences ($p<0.0001$). Data were collected from three independent experiments and 31–60 germlines were scored for each genotype. (**D**) SPC zone length after knocking down CCR4-NOT subunits in the *fbf-1(lf) fbf-2(lf); gfp::fbf-1(fbf-2vr4)* and *fbf-1(lf) fbf-2(lf); gfp::fbf-1(fbf-2vr3)* genetic backgrounds (as indicated on the X-axis). Plotted values are means ± SD. Asterisks mark the group with significant changes in SPC zone length after CCR4-NOT knockdown vs control RNAi by one-way ANOVA ($p<0.01$). Data were collected from two independent experiments. *N*, the number of hermaphrodite germlines scored. (**B–D**) All experiments were performed at 24°C.

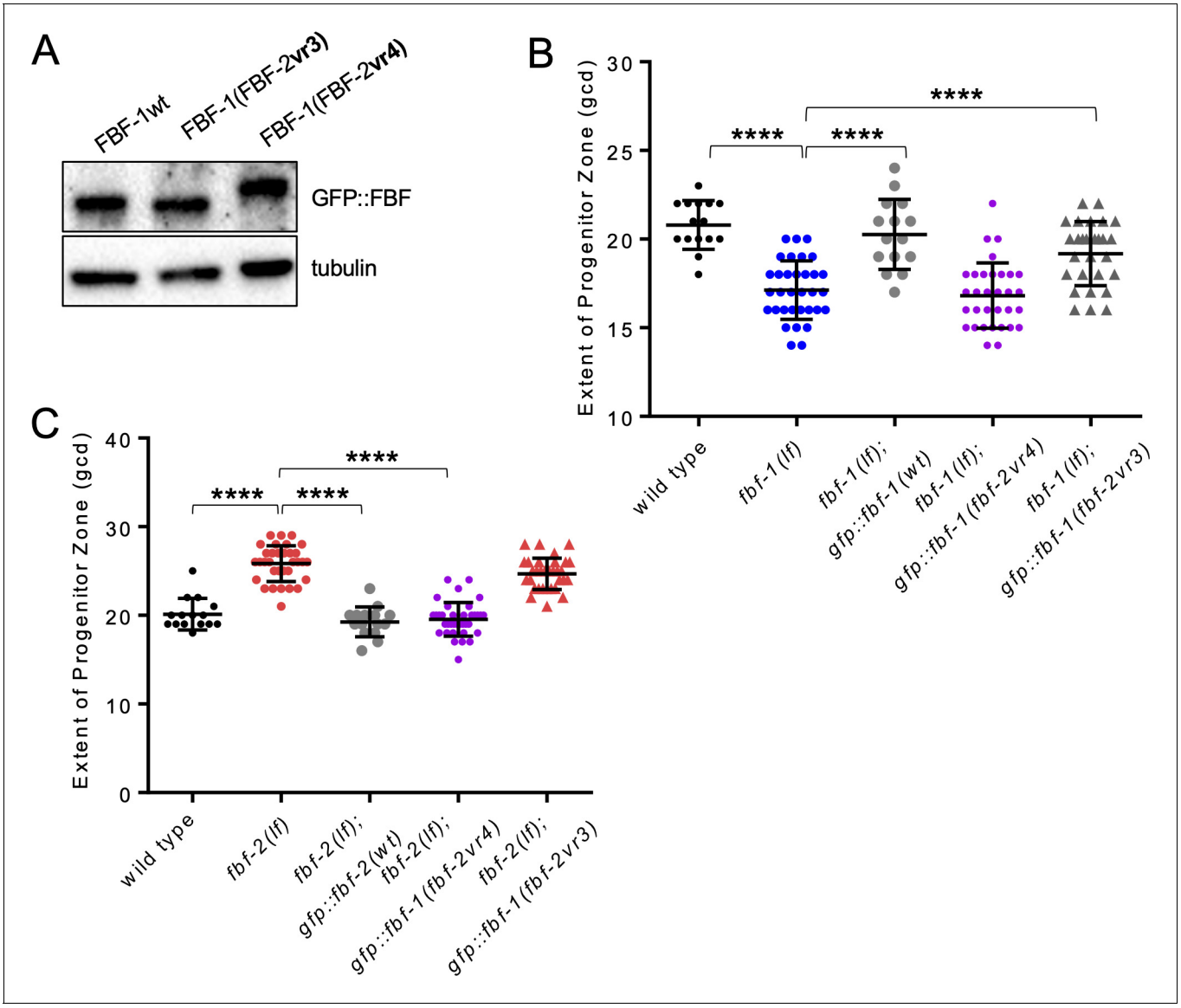

Figure 7—figure supplement 1. Variable region 4 of FBF-2 allows chimeric FBF-1vr4 to rescue *fbf-2(lf)*. (**A**) Expression levels of GFP::FBF-1(wt), GFP::FBF-1(FBF-2vr3), and GFP::FBF-1(FBF-2vr4) transgenes assessed by a western blot. Tubulin is used as a control. (**B**) SPC zone length was measured after crossing GFP::FBF-1(FBF-2vr4), GFP::FBF-1(FBF-2vr3) and GFP::FBF-1(wt) transgenes into *fbf-1(lf)* genetic background. As controls, the extent of SPC zone was also measured in *fbf-1(lf)* and the wild type. (**C**) SPC zone length was measured after crossing GFP::FBF-1(FBF-2vr4), GFP::FBF-1(FBF-2vr3) and GFP::FBF-2(wt) transgenes into *fbf-2(lf)* genetic background. As controls, SPC zone length was also measured in *fbf-2(lf)* and the wild type. (**B, C**) Plotted values are individual data points and means ± SD. Differences in the extent of SPC zone between *fbf-1(lf)* or *fbf-2(lf)* and all other strains in a given group were evaluated by one-way ANOVA test with Dunnett's post-test; asterisk marks statistically significant differences ($p<0.0001$). Data were collected from two independent experiments with 7–20 germlines scored for each genotype per replicate. (**A–C**) All experiments were performed at 24°C.

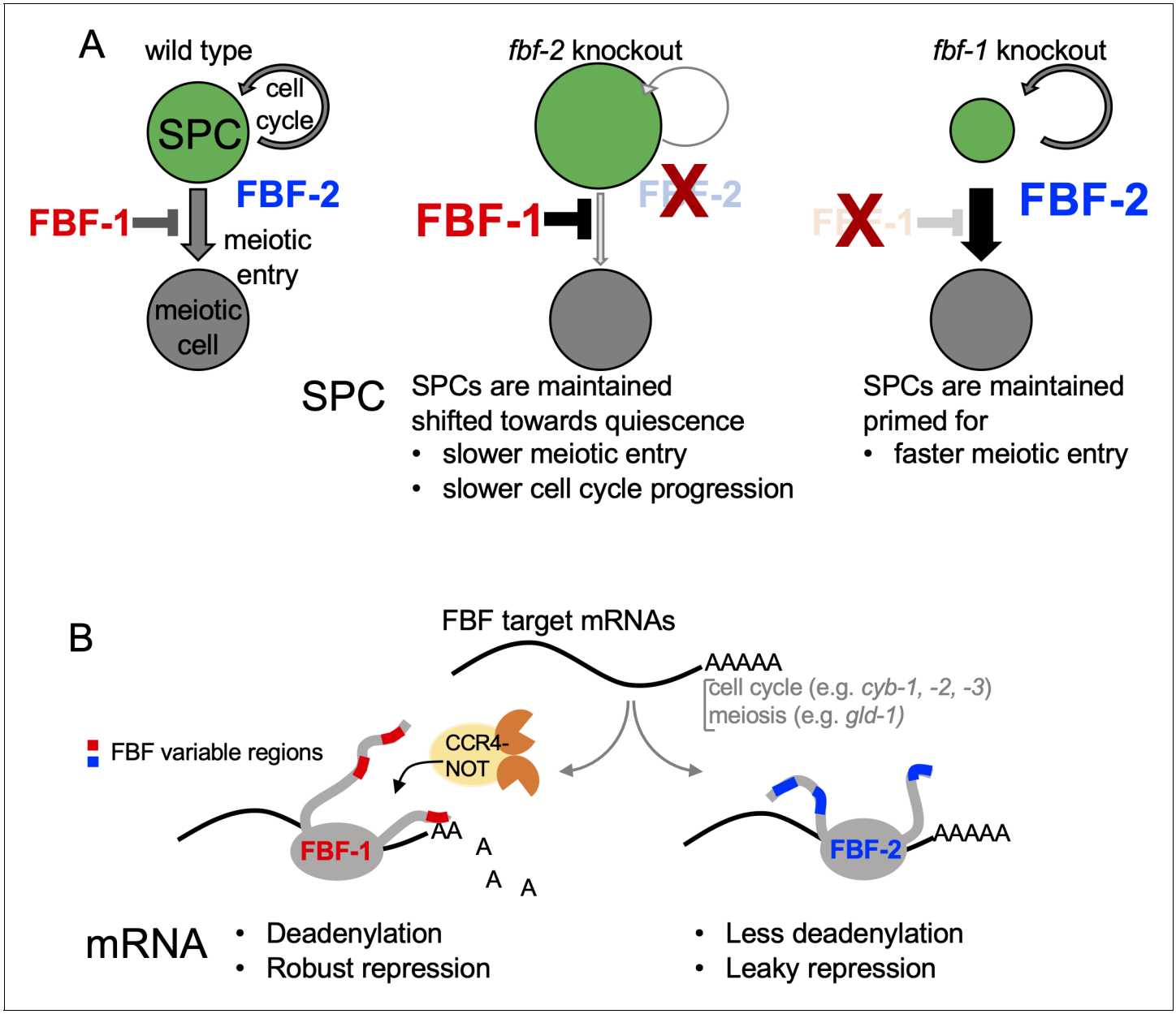

Figure 8. A model of antagonistic effects of FBF-1 and FBF-2 on germline SPC dynamics and target mRNAs. (**A**) FBFs regulate the rate of stem and progenitor (green) cell division and the rate of entry into meiosis (grey). Both FBFs negatively regulate each other's expression (***Lamont et al., 2004***, not pictured). In *fbf-2(lf)*, FBF-1 is overexpressed, and both cell division and meiotic entry rates are slow. This results in an increased total number of SPCs in the adult (larger green circle). In *fbf-1(lf)*, FBF-2 is overexpressed and meiotic entry rate is enhanced, reducing overall numbers of SPCs (smaller green circle). In the double *fbf-1(lf) fbf-2(lf)* mutant (not pictured), adult SPCs are lost to differentiation. (**B**) FBF-1 and FBF-2 bind the same target mRNAs, and each can promote SPC maintenance. FBF-1 cooperates with CCR4-NOT deadenylase and robustly represses target mRNAs (***Crittenden et al., 2002***; ***Brenner and Schedl, 2016***) to restrict the rate of germline stem cell meiotic entry. FBF-2 protects mRNAs from deadenylation; FBF-2-dependent regulation is associated with leaky repression of protein synthesis and sustains the wild-type rates of SPC cell division and meiotic entry. Differential cooperation of FBFs with CCR4-NOT is determined by their variable regions outside of the RNA-binding domain.